THE ASTROPHYSICAL JOURNAL, 408:92–107, 1993 May 1

THE HOT STELLAR COMPONENT IN ELLIPTICAL GALAXIES AND SPIRAL BULGES. I. THE FAR-ULTRAVIOLET SPECTRUM OF THE BULGE OF M31

HENRY C. FERGUSON
University of Cambridge, Institute of Astronomy, The Observatories, Madingley Road, Cambridge CB3 0HA, England
AND
ARTHUR F. DAVIDSEN
Center for Astrophysical Sciences, Henry A. Rowland Department of Physics and Astronomy, The Johns Hopkins University, Baltimore, MD 21218
Received 1992 July 31; accepted 1992 October 23

ABSTRACT

We present a spectrum of the bulge of M31 from 1850 Å to the Lyman limit measured through a 9″ × 116″ aperture by the Hopkins Ultraviolet Telescope (HUT) during the Astro-1 space shuttle mission in 1990 December. Apart from airglow, no significant emission features are present in the spectrum. A search for stellar absorption features reveals several significant detections, but uncertainties in the interstellar-medium contribution and the temperatures of the stars contributing to the spectrum preclude any definite conclusions about the metallicity of the stellar population.

We compare the HUT spectra of the M31 bulge and of NGC 1399, the central giant elliptical in the Fornax Cluster. We find significant differences that are relatively insensitive to the assumptions about extinction. Evidently the stars producing the far-UV upturn in UV-bright galaxies such as NGC 1399 are not just more of the same stars producing the emission in UV-fainter galaxies like M31.

We investigate the possibility that the two spectral-energy distributions (SEDs) differ only in the fractional contribution from classical post–asymptotic giant branch (PAGB) stars and in the amount of extinction. We find an acceptable fit to the M31 spectrum for $E(B-V) = 0.11$ if $\sim$65% of the flux (at $\sim$1400 Å) comes from PAGB stars and the rest comes from stars of the type producing the far-UV emission in NGC 1399. The *known* PAGB population from optical observations (central stars of planetary nebulae) can account for less than 1% of the total far-UV flux. The pointlike sources recently detected at 1750 Å by the *HST* Faint Object Camera are probably PAGB stars with masses lower than planetary-nebula central stars (thought to be $\sim$0.6 $M_\odot$). These sources too appear to account for only a small fraction ($\sim$15%) of the flux observed by HUT at 1750 Å. These results suggest that PAGB stars with still lower masses, which would be fainter than the FOC detection limit for point sources, contribute to the M31 SED.

We examine the hypothesis that the UV continuum in both galaxies is dominated by stars in post-horizontal branch (post-HB) phases of evolution, with a distribution of post-HB masses governed by the mean metallicity and metallicity spread of the population. The number of UV photons produced per star increases toward lower mass, while the characteristic temperature of the UV emitting population decreases. In this scenario, the far-UV flux of NGC 1399 is produced mostly by low-mass extreme horizontal branch, post-early-AGB, and/or AGB-Manqué stars, while in M31 there is a large contribution from classical PAGB stars as well. We can thus qualitatively explain both the relative fluxes of the UV rising branches in NGC 1399 and M31, and the shapes of their SEDs. This scenario makes a prediction, which we confirm from existing surveys, that the number of planetary nebulae per unit luminosity is anticorrelated with the strength of the UV upturn. It also makes testable predictions for the far-UV SEDs of low-metallicity ellipticals and the spectral evolution of giant ellipticals.

Subject headings: galaxies: individual (M31, NGC 1399, M32) — galaxies: stellar content

1. INTRODUCTION

The bulge of M31 is one of the key testing grounds for theories of the evolution of old, metal-rich stellar populations. In contrast to the Galactic bulge, M31 is sufficiently far away and free from Galactic extinction that spectral synthesis techniques used for more distant galaxies can be applied over a large range of wavelengths, yet is sufficiently nearby that the spectral synthesis results can be directly compared with color-magnitude diagrams. The spectral energy distribution of the M31 bulge resembles that of more distant ellipticals, and the bulge falls nicely on the metallicity-luminosity and color-luminosity correlations for giant ellipticals, giving us some confidence that both the formation process and the present-day stellar populations are similar.

One of the least well understood stellar populations in such systems are the hot stars that produce the far-ultraviolet continuum seen by the *OAO 2*, *ANS*, and *IUE* satellites (Code & Welch 1979; de Boer 1982; Johnson 1979; Perola & Terenghi 1980; Nørgaard-Nielsen & Kjægaard 1981; Bertola, Capaccioli, & Oke 1982; Burstein et al. 1988; Buson, Bertola, & Burstein 1990). Galaxies with similar luminosities and optical spectra are observed with UV-to-optical flux ratios that vary by an order of magnitude. This wide variation, coupled with our complete ignorance of the evolution of the UV component, constitutes a major uncertainty in the interpretation of the counts and colors of high-redshift galaxies (Bruzual 1983; Yoshii & Takahara 1988; Sandage 1988). Identifying the source of the UV emission in nearby galaxies thus has impor-

tant consequences for cosmology, as well as for our understanding of late phases of stellar evolution (Greggio & Renzini 1990; Castellani & Tornambè 1991; Horch, Demarque, & Pinsonneault 1992).

To study the UV upturn in more detail, we observed the elliptical galaxy NGC 1399 and the M31 bulge with the Hopkins Ultraviolet Telescope (HUT) during several periods of orbital night during the 9 day Astro-1 space shuttle mission. HUT is capable of obtaining one-dimensional spectra with high sensitivity and moderate spectral resolution ($R \sim 400$) in the 850–1850 Å bandpass. The large projected size of the spectrograph aperture offers considerable grasp for extended sources, such as nearby galaxies. NGC 1399 is the "quiescent" galaxy with the bluest 1550 Å $- V$ color in the Burstein et al. (1988) survey. It is a normal luminous elliptical in many respects, although it does sit at the center of the Fornax Cluster, is a low-luminosity radio source, and has a massive X-ray halo (none of which are particularly unusual for a galaxy of its luminosity). M31 has a less pronounced UV upturn, but it follows the elliptical-galaxy correlations of UV color with metallicity and velocity dispersion very well (Burstein et al. 1988).

The preponderance of observational evidence, reviewed by Burstein et al. (1988), Greggio & Renzini (1990) and Davidsen & Ferguson (1993), suggests that the UV flux in quiescent ellipticals comes from an old stellar population, rather than from recent star formation. The strong correlation of 1550 Å $- V$ color with Mg_2 index (Burstein et al. 1988) suggests that metallicity may be the driving parameter that influences strength of the UV upturn. Until recently, post-asymptotic giant branch (PAGB) stars have seemed the most likely candidate because of their high temperatures and luminosities, and because of the strong dependence of their fuel consumption on mass (Bohlin et al. 1985; Mochkovitch 1986; Burstein et al. 1988; Barbaro & Olivi 1989; Bertelli, Chiosi, & Bertola 1989). By PAGB stars, we are referring to stars that reach the peak luminosity of the AGB before evolving to higher temperatures. The evolution from the AGB to the PAGB phase is governed almost entirely by mass-loss processes, which are very poorly constrained both theoretically and observationally. At the tip of the AGB, stars undergo thermal pulses (Iben & Renzini 1983), and, depending on mass loss, may leave the AGB either during a thermal pulse, in which case they derive most of their subsequent UV luminosity from helium-shell burning (Wood & Faulkner 1986), or between two thermal pulses, in which case they derive most of their UV luminosity from hydrogen-shell burning (Schönberner 1983). Models for low-mass PAGB stars exist only for the hydrogen-burning case, although a comparison of the properties of both types can be made for masses above 0.6 $M_\odot$ (Wood & Faulkner 1986; Greggio & Renzini 1990).

Recent critical examination of the total fuel consumption at high temperatures suggests that these "classical" PAGB stars cannot deliver sufficient energy to produce the strongest observed UV upturns (Brocato et al. 1990; Greggio & Renzini 1990; Castellani & Tornambè 1991; Castellani, Limongi, & Tornambè 1992). In particular, to account for the strong UV upturns seen in giant ellipticals like NGC 1399, it is necessary to extrapolate the trend of increasing fuel consumption with decreasing mass to still lower masses (Burstein et al. 1988; Bertelli, Chiosi, & Bertola 1989). Greggio & Renzini (1990) questioned the validity of this extrapolation, and more recent PAGB models (Castellani & Tornambè 1991) suggest that even low-mass PAGB stars cannot produce sufficient UV luminosity. More attractive candidates are extreme horizontal branch (EHB) stars; post-early-AGB (PEAGB) stars, which leave the AGB before reaching the thermally pulsing phase; and AGB-Manqué stars, which evolve directly to high temperatures from the horizontal branch, skipping the AGB phase entirely (Greggio & Renzini 1990; Castellani & Tornambè 1991; Horch et al. 1992). These candidates may produce many more UV photons per star than classical PAGB stars; however, whether or not they actually exist remains a subject of speculation.

Observations of NGC 1399 with HUT (Ferguson et al. 1991) have provided observational evidence against PAGB stars as the dominant source of the UV emission in galaxies with the strongest upturns. Ferguson et al. (1991) constructed synthetic spectra of PAGB star populations evolving along the Schönberner (1983, 1987) tracks with standard solar-metallicity atmospheres (Kurucz 1991; Clegg & Middlemass 1987), and showed that these produced a poor fit to the HUT data. In particular, the characteristic temperature of the model population was too hot to explain the fairly pronounced turnover near the Lyman limit in the NGC 1399 spectrum. This finding does not exclude the possibility that PAGB stars with masses lower than the lowest Schönberner track (0.546 $M_\odot$) produce most of the far-UV emission. Two effects will lower the flux near the Lyman limit in such populations. First, the peak temperature reached along the PAGB track decreases with decreasing mass, and second, if the population is metal-rich, the line blanketing is presumably underestimated by the solar-metallicity atmospheres used for the synthetic spectra. Nonetheless, the change must be fairly dramatic over a small change in mass and metallicity for classical PAGB models to survive.

In this paper, we present an analysis of the M31 spectrum and compare it to NGC 1399. There are significant differences between the two spectra that cannot easily be explained by uncertainties in extinction. The M31 spectrum requires a contribution from stars hotter than those that dominate the NGC 1399 SED. We find that we can produce an acceptable fit to the M31 spectrum by assuming that it consists of stars like those in NGC 1399, combined with a much higher proportion of classical PAGB stars. This result is not completely conclusive because of uncertainties in extinction, but it agrees with the idea that as metallicity increases so does the contribution from EHB, PEAGB, and AGB-Manqué stars (which spend more time at lower temperatures than PAGB stars and produce more photons in the HUT spectral range).

The observations and data reduction are described in § 2. The problems of extinction and contamination from the M31 disk are considered in § 3. In § 4 we compare our data to *IUE* and find reasonable agreement, albeit with a zero-point shift that is consistent with a UV color gradient in the M31 bulge. Emission and absorption features are discussed in § 5. The comparison to NGC 1399 is presented in § 6. In § 7 we develop a two-component model for the M31 SED and estimate the contribution of PAGB stars to the UV light. We discuss the known PAGB star population (the central stars of planetary nebulae and the point sources recently resolved with the *HST* Faint Object Camera) in § 8. In § 9 we consider a unified scenario along the lines suggested by Greggio & Renzini (1990), wherein the UV upturn is produced by various populations of evolved metal-rich stars whose proportions depend on metallicity and metallicity spread. This scenario can qualitatively explain both the relative fluxes of NGC 1399 and M31 and the

differences in their SED's. It also predicts an inverse correlation in the number of planetary nebulae (PN) per unit luminosity with the strength of the UV upturn. Examination of existing PN data confirms that such a correlation exists. A summary of our principal conclusions is given in § 10.

2. OBSERVATIONS

HUT observed the bulge of M31 for 3006 s on 1990 December 6 through a 9.″4 × 116″ aperture centered on the nucleus at a position angle of 25°. The observation took place partly during orbital day and partly during the night. Because the airglow contamination is greatly reduced on the night side of the orbit, we consider here only a 2288 s segment of night data.

The HUT experiment, its performance in orbit, and its initial calibration are described by Davidsen et al. (1992). The raw M31 spectrum is shown in Figure 1. To produce the flux-calibrated spectrum we subtracted dark counts and scattered light (determined from a region free from airglow lines below 912 Å), corrected the observed count rate for phosphor persistence (a uniform 5% correction), divided by the HUT effective area (Davidsen et al. 1992), and corrected for a slight off-axis sensitivity variation (a 5% effect at 1800 Å, decreasing to less than 1% below 1500 Å). The resultant spectral energy distribution after airglow subtraction (see below) is shown in Figure 2. The spectrum longward of 1824 Å contains a small contribution from the second-order galaxy continuum longward of 912 Å. We have not corrected for this, but use only the spectrum shortward of 1820 Å in our analysis. The uncertainties in the instrumental corrections are small compared to the uncertainty in the extinction discussed in § 3. The HUT sensitivity calibration is tied to a model atmosphere for the DA white dwarf G191 − B2B, and is believed to be accurate to better than 10% from comparison to pre- and post-flight laboratory calibrations (Davidsen et al. 1992; Kimble et al. 1993). The NGC 1399 spectrum presented here for comparison to M31 is slightly revised from Ferguson et al. (1991) by the use of an updated sensitivity curve and revision of the correction for off-axis sensitivity variation. The largest change is 8% at 1780 Å, and is generally much smaller than that; our previous conclusions are therefore unaffected.

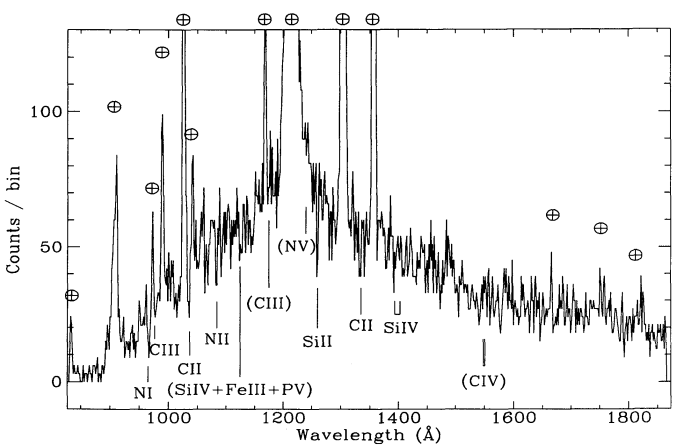

FIG. 1.—HUT spectrum of the M31 bulge from 2288 s of observations on the night side of the orbit. The spectrum has been binned over three instrumental pixels corresponding to 1.5 Å (half the instrumental resolution). All of the emission features are due to airglow. We have marked positions (⊕) of the strongest expected absorption features from the stellar population or interstellar medium (excluding those that are obscured by the airglow, e.g., the Lyman series). Features that are not detected at greater than 3 σ are marked in parentheses.

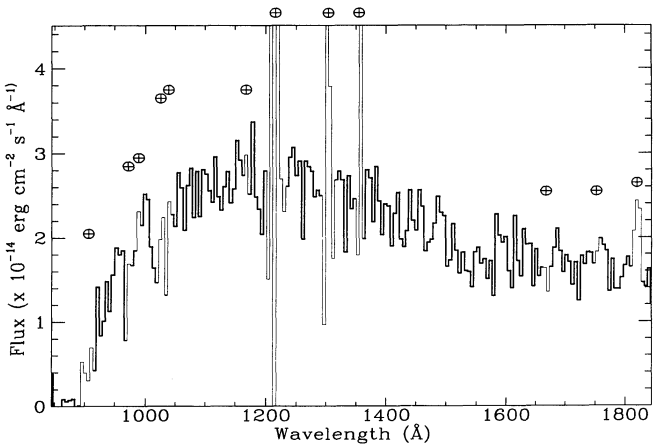

FIG. 2.—Flux-calibrated, airglow-subtracted HUT spectrum of the M31 bulge, binned to 5 Å. Places where airglow has been subtracted are marked by ⊕, and the data are plotted with a lighter line in these regions.

The most prominent features in the raw M31 spectrum are the emission lines from the Earth's upper atmosphere. The relative strengths of these lines vary with orbital position and viewing direction, making them difficult to subtract entirely. To estimate the airglow contribution we have fit profiles of the individual features in a blank night-sky spectrum taken through the 9″ × 116″ aperture. We then (in most cases) held the line profiles fixed and found the best-fit of a continuum plus airglow model to regions around the individual airglow lines. The nonlinear curve-fitting package "specfit," written by G. Kriss, was used within IRAF[1] to minimize χ^2 for this and all subsequent model fitting in this paper. Uncertainties were taken to be Poisson due to counting statistics alone. This is a slight underestimate because there are calibration uncertainties, and there are small (less than 2%) pixel-to-pixel variations in sensitivity.

Details of the line fitting are given in Table 1. The Lyα and O I λ1304 lines are so strong that counting statistics preclude their clean subtraction. Because of the uncertain nature of the airglow subtraction, we have carefully avoided regions affected by strong features (near 1026, 1216, 1304, and 1356 Å) in fitting models to the SED.

3. CORRECTION FOR EXTINCTION AND DISK CONTAMINATION

The largest uncertainty in the M31 UV spectral-energy distribution is the correction for extinction. Values for the mean reddening range from $E(B-V) = 0.04$ (Tully 1988), to 0.11 (McClure & Racine 1969). Burstein et al. (1988) assumed $E(B-V) = 0.08$ in their analysis of the *IUE* observations. For most of our discussion we have adopted the higher value of 0.11, based on star counts, which was used in the earlier analysis of the *IUE* data by Welch (1982) and was adopted by Ciardullo et al. (1989b) in their analysis of the planetary nebula luminosity function. Nevertheless, we regard the amount of extinction as uncertain in our analysis, and consider various values for $E(B-V)$ in the model fitting discussed below. The

[1] IRAF is distributed by Kitt Peak National Observatory, National Optical Astronomy Observatories, operated by the Association of Universities for Research in Astronomy, Inc., for the National Science Foundation.

TABLE 1

AIRGLOW FEATURES IN M31 SPECTRUM

Vacuum (Å)	Feature	Best-Fit (Å)	Total Counts	Wavelength Range for Fit	Comments
911	O I	910.43	286	890–920	Skewed line profile. Shape in M31 spectrum is quite different from blank-sky spectrum. Shape and width allowed to vary in fit. Flux contribution drops to less than 20% by 925 Å.
972.54	H I Lyγ	973.4	49	949–962 971–976 979–984	Avoided possible absorption lines at 966 and 977 Å. Possibly affected by intrinsic M31 Lyγ and C III absorption.
988.6–990.8	O I	989.65	103	980–1000	
1025.7–1028.2 1025.72	O I + H I Lyβ	1026.27	363	1000–1030	Probably affected by intrinsic M31 Lyβ absorption.
1039.2–1041.7	O II	1041.17	41.5	1038–1050	Probably affected by M31 C II absorption.
1134.2–1135.0	N I	1134.63	4	1120–1148	
584.33 × 2	He I	1168.61	109	1145–1173	
1215.67	H I Lyα	1215.82	165438	1100–1129 *c* 1140–1163 *c* 1313–1350 *c* 1180–1210 *l* 1121–1252 *l*	Completely obliterates intrinsic M31 Lyα absorption. *c* = used to set continuum *l* = used to fit line center and flux
1302.2–1306.0	O I	1305.2	3640	1270–1320	Possibly affected by intrinsic M31 Si III absorption
1355.6–1358.5	O I	1355.92	895	1339–1375	
(834.8–834.5) × 2	O I	1666.29	23	1648–1688	
584.33 × 3	He I	1751.54	16	1732–1772	

uncertainty in the shape of the far-UV extinction curve introduces an additional complication that we have not attempted to model. In all cases we have used the Seaton (1979) extinction curve, assuming it is valid to the Lyman edge, as indicated by *Voyager* observations (Longo et al. 1989).

In addition to Galactic extinction, there is probably further attenuation by the interstellar medium within M31. Images of the bulge of M31 show dust features extending all the way into the nucleus (Kent 1983). The mean reddening is less than $E(B-V) = 0.03$ in the HUT slit, but it is clearly quite patchy. Because the effects of patchy obscuration are difficult to model and because the effect is probably quite small, we have not made any correction for internal extinction in M31, but consider its possible effects when comparing the spectrum to NGC 1399.

An additional source of uncertainty is the contribution from the M31 disk population in the HUT aperture. Ultraviolet images of the M31 bulge fail to detect point sources corresponding to massive main-sequence stars (Bohlin et al. 1985; O'Connell 1991), so we have assumed that disk contamination is negligible. The resultant flux calibrated spectrum corrected for $E(B-V) = 0.11$ is shown in Figure 3.

4. COMPARISON TO *IUE*

Table 2 lists the observed and reddening-corrected mean flux of M31 in 50 Å intervals in the HUT 9.″4 × 116″ aperture. The errors from counting statistics are less than 5%, and are therefore comparable to the errors due to calibration uncertainties and airglow subtraction. In computing the means in Table 2, we have avoided regions contaminated by strong airglow lines. For comparison, Table 2 also gives the observed SED of NGC 1399 (shifted to rest wavelength), with no extinction correction applied. For M31, Welch (1982) gives a similar tabulation for the *IUE* observations. The mean flux ratio is $f_{HUT}/f_{IUE} = 2.56$ and the standard deviation of this ratio over

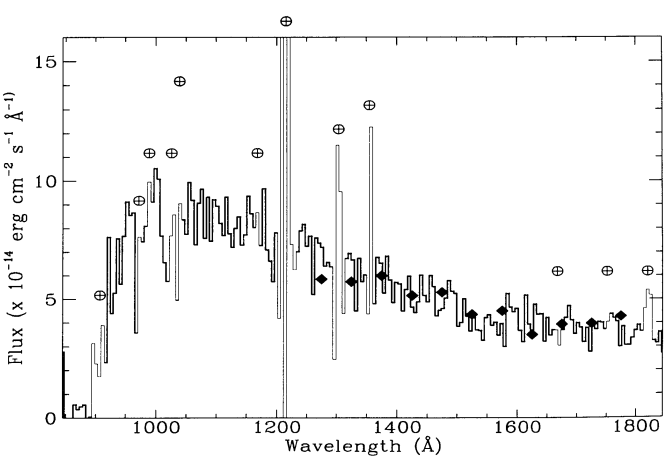

FIG. 3.—Flux-calibrated, airglow-subtracted HUT spectrum of the M31 bulge, binned to 5 Å, corrected for extinction assuming $E(B-V) = 0.11$. The diamonds show the *IUE* observations from Welch (1982) with the same extinction correction applied, scaled upwards by a factor of 2.56, the mean ratio of HUT/*IUE* flux from 1250–1800 Å. This scale factor is consistent with the aperture ratio of the two instruments and the far-UV surface-brightness profile of M31 obtained by UIT.

TABLE 2

SPECTRAL ENERGY DISTRIBUTIONS OF M31 AND NGC 1399

Wavelength (Å)	Observed M31 Flux ($\times 10^{14}$ ergs cm^{-2} s^{-1} Å^{-1})	Reddening-corrected M31 Flux ($\times 10^{14}$ ergs cm^{-2} s^{-1} Å^{-1})	NGC 1399 Flux ($\times 10^{14}$ ergs cm^{-2} s^{-1} Å^{-1})
925.....	1.15	5.91	0.69
975.....	1.85	8.43	1.66
1025.....	2.08	8.11	2.11
1075.....	2.52	8.65	2.29
1125.....	2.60	8.07	2.17
1175.....	2.71	7.82	2.22
1225.....	2.57	6.95	1.89
1275.....	2.62	6.82	1.94
1325.....	2.49	6.17	1.63
1375.....	2.49	6.00	1.41
1425.....	2.21	5.22	1.23
1475.....	2.20	5.13	1.18
1525.....	1.73	4.00	0.92
1575.....	1.81	4.17	0.90
1625.....	1.77	4.03	0.82
1675.....	1.71	3.85	0.86
1725.....	1.65	3.67	0.71
1775.....	1.65	3.63	0.76

50 Å intervals from 1250 to 1800 Å is 0.25, consistent with expectations from the combined calibration uncertainties of HUT and *IUE*. The *IUE* SED, corrected for extinction and scaled by a factor of 2.56, is shown in Figure 3.

For comparison, we have computed the HUT/*IUE* flux ratio expected if the UV follows the optical surface-brightness profile. We used Kent's (1983) surface photometry to construct a two-dimensional model using the STSDAS isophote package (Jedrzejewski 1987), and then computed the ratio of the optical flux in the HUT and *IUE* apertures by summing over the pixel intensities within the two apertures in the model image. For *IUE*, we have assumed a rounded 10″ × 20″ aperture constructed of a central 10″ × 10″ square with two semicircles of radius 5″ on either end. The actual geometry is uncertain, since it depends on how the spectrum was extracted and on vignetting within the instrument. Similarly, the HUT flux may be slightly underestimated because of vignetting, and because pointing system problems during the Astro-1 mission often allowed targets to wander about a bit in the aperture. Nevertheless, the expectation for the nominal aperture sizes and stable pointing is that the flux ratio should be $f_{HUT}/f_{IUE} = 3.30$ if the UV follows the optical profile. The HUT aperture is nearly as wide as *IUE*'s, but is much longer. Therefore, the lower-than-expected HUT flux suggests that the far-UV light is more centrally concentrated than the optical. This is in agreement with the results from *IUE* and imaging experiments (Welch 1982; Deharveng et al. 1982; Bohlin et al. 1985). To compare directly to the recent UIT results (O'Connell et al. 1992), we have computed the expected flux through the HUT and *IUE* apertures from the surface-brightness profile in the UIT 1520 Å bandpass (O'Connell 1992). The result, $f_{HUT}/f_{IUE} = 2.67$, is compatible with the observed flux ratio, considering the uncertainties in pointing and in the geometry of the apertures. This agreement between different instruments adds confidence to the relative calibration of HUT and *IUE*, and to the conclusion that there is a steep rise in the UV/optical flux ratio toward the center of M31.

5. EMISSION AND ABSORPTION FEATURES

Apart from the airglow lines, no significant emission features are seen in the HUT spectrum of M31. We have estimated upper limits for the C IV λλ1548, 1550, and the He II λ1640 lines by fitting a linear continuum to 30 Å regions of the spectrum around the expected features, then adding Gaussian lines whose width is equal to the instrumental profile until $\Delta\chi^2$ exceeds 2.7 (90% confidence interval). The flux limits are 2.7×10^{-14} ergs cm^{-2} s^{-1} for C IV and 2.3×10^{-14} ergs cm^{-2} s^{-1} for He II. For C IV, the 1 σ upper limit given by Welch (1982) is 6.3×10^{-15} ergs cm^{-2} s^{-1}, measured through the 10″ × 20″ *IUE* aperture. Translated into a mean surface brightness, the HUT upper limit, 2.5×10^{-17} ergs cm^{-2} s^{-1} arcsec^{-2}, is slightly lower than that from *IUE*, and comparable to the expected flux from known planetary nebulae in M31, as discussed in § 8.

Given the modest signal-to-noise ratio in the HUT spectrum, absorption features are not readily visible. The strongest expected stellar features are the Lyman series lines (clearly visible in the NGC 1399 spectrum), which in M31 are unfortunately masked by the Lyman series emission lines in the airglow. Longward of Lyα the strongest expected absorption lines, if the stellar population is hotter than $T_{eff} \sim 25000$ K, are N V λλ1239, 1243, Si IV λλ1394, 1403, and C IV λλ1548, 1550. If cooler stars dominate, Si II + Si III λ1300–1304, C II λ1335, and Si II λ1260 might appear (Snow & Morton 1976; Walborn, Nichols-Bohlin, & Panek 1985; Welch 1982). All these are possible interstellar lines as well, so detection does not automatically constrain the stellar population. Shortward of Lyα the absorption line density becomes so high (several per Å) that identifying individual features at the HUT resolution is even more difficult. Other than the Lyman series, the most obvious individual features should be C III λ1175, Si IV + P V + Fe III at λ ~ 1125, N II λ1085, C II λλ1036, 1037, O VI λλ1032, 1038, and C III λ977. The only feature clearly visible in the M31 spectrum that is *not* expected in the atmospheres of hot stars is the line at 965 Å, which we tentatively identify as interstellar N I.

To estimate absorption-line strengths or upper limits, we have fit Gaussian absorption lines plus a linear continuum to small regions around the wavelengths of the expected features in the raw spectrum. Near airglow lines, we have used the best-fit line profiles from a blank-sky spectrum to fit the emission lines as well, allowing shifts in wavelength and normalization to find the best fit when combined with the absorption

features. We used the vacuum wavelengths of the expected features as first guesses, but left the wavelength as a free parameter in the fit for three reasons: (1) many of the lines are blends, (2) we don't know a priori whether a given feature is associated with M31 or the intervening Galactic ISM, and (3) pointing errors may shift the apparent wavelengths of M31 features slightly. Where multiple features were fit simultaneously, we held the ratios of the wavelengths of the different features fixed. Line widths were fixed at the instrumental resolution, except for the 965 and 1036 Å features, which are close blends that we fit with one line allowing the width to vary, and Lyβ and Lyγ, which could in principle be so strong that they have very broad wings. Table 3 lists the results of the absorption-line fitting. Uncertainties were estimated by progressively lowering the equivalent width until $\Delta\chi^2$ exceeded the 68% confidence interval from the best fit. The fifth column lists the formal probability that each feature results from a statistical fluctuation in a pure continuum.

The C IV feature is detected at the 99% confidence level, but shifted about 6 Å from its expected wavelength at the radial velocity of M31. Inspection of the *IUE* Atlas of O-Type Spectra (Walborn et al. 1985) reveals that shifts to the blue of up to 10 Å are not uncommon, even among main-sequence O stars. These shifts are undoubtedly due to winds, but the emis-

TABLE 3

ULTRAVIOLET ABSORPTION LINES IN M31

Species	Wavelength (lab)	Wavelength (measured)	E.W. (Å)	Significance	χ^2	ν
N I	965	966.6	2.6 ±0.4	3.1 ×10^{-6}	44.7	47
H I	972.5	971.6	2.1 ±1.8	1.1 ×10^{-1}		
C III	977.0	976.9	1.3 ±0.5	9.5 ×10^{-3}		
H I	1025.7	1024.5	5.5 ±1.8	1.1 ×10^{-2}	86.5	66
C II + O VI	1037	1035.5	1.7 ±0.4	3.9 ×10^{-4}		
N II	1084	1082.6	1.4 ±0.4	1.8 ×10^{-4}	79.0	55
Si IV	1122.5	1121.4				
Fe III	1125.7	1124.9	1.2 ±0.5	4.8 ×10^{-2}	68.4	55
P V	1128.0	1128.0				
C III	1175.7	1174.0	0.5 ±0.5	1.6 ×10^{-1}	76.4	72
N V	1240	1236.5	1.6 ±0.7	1.5 ×10^{-2}	28.3	36
Si II	1260.4	1259.8	1.5 ±0.3	3.0 ×10^{-6}	60.4	37
C II	1334.5	1333.7	1.3 ±0.3	6.3 ×10^{-4}	72.9	54
C II	1335.7	1334.9				
Si IV	1393.7	1392.3	1.0 ±0.5	4.2 ×10^{-3}	50.5	53
Si IV	1402.8	1401.3	0.2 ±0.4	5.1 ×10^{-1}		
C IV	1548.2	1540.5	1.6 ±0.6	9.1 ×10^{-3}	59.3	58
C IV	1550.8	1543.1				

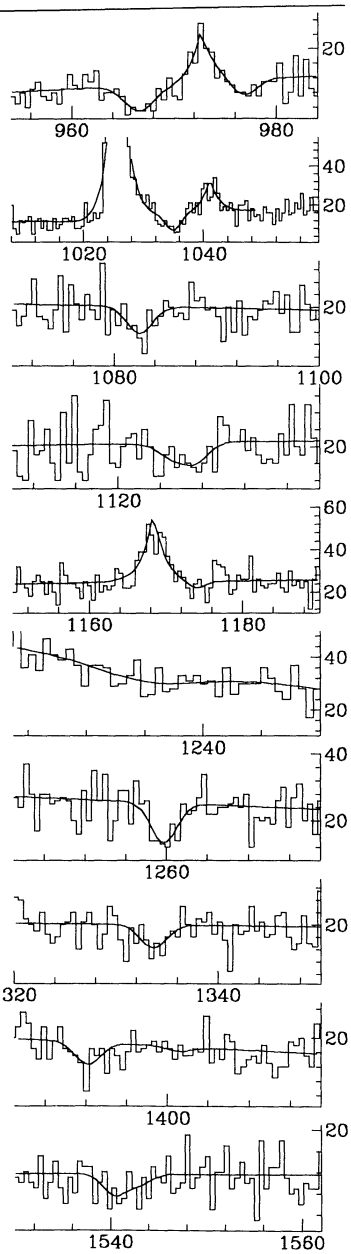

sion component of a P Cygni profile is frequently not present in late O-type dwarfs, and in most cases the Si IV lines do not shift appreciably. Therefore the detection of a feature due to C IV at ~1542 Å in the HUT spectrum of M31 seems plausible, if not highly significant statistically. Note that the C IV absorption, even if detected, is much weaker than expected from ongoing star formation with a standard IMF (Ferguson et al. 1991; Rocca-Volmerange & Guiderdoni 1987), and indeed is weaker than expected from a combination of solar-metallicity dwarfs that matches the continuum shape (see below). The 1036 Å feature seems more consistent with C II than O VI given the wavelength and width of the detected feature.

The lines most clearly identified in the spectrum are C II λ1335 and Si II λ1260. These lines are well separated from airglow, and are less affected by the difficulty in assigning a true continuum level than features below Lyα. Both lines are often strong interstellar absorption features. Given the uncertainty in the density and velocity distribution of gas along the line of sight, it is difficult to tell how much the ISM contributes. For the range of $E(B-V)$ from 0.04 to 0.11, with standard dust-to-gas ratios and solar-system abundances, the contribution could be anywhere from one-third to the entire equivalent widths of the two lines. If the ISM contribution is large, then the intrinsic stellar absorption lines must be weak.

On the basis of the absorption lines seen in the *IUE* spectrum, Welch (1982) argued that the dominant UV-emitting population in M31 must be metal-poor. The strongest absorption features in the *IUE* spectrum were the 1260 and 1335 Å features just discussed, and the 1302 Å Si II + Si III blend. While the latter falls under the strong O I airglow feature in our spectrum, the *IUE* equivalent widths of the two other features are consistent with our estimates from the HUT spectrum. Because C IV and Si IV are weak, Welch (1982) ruled out a significant contribution from main-sequence stars of spectral type earlier than B2. For stars between B2 and B7, he finds the equivalent width of the 1302 Å feature is at least twice that seen in M31. The 1260 and 1335 Å features become too strong in spectral types later than B4. However, the line strengths appeared to match those of evolved low-metallicity stars quite well.

While our spectrum confirms the absorption-line detections and relative weakness of the C IV and Si IV features in the *IUE* spectrum, we do not believe that the line strengths uniquely implicate metal-poor stars as the dominant population. In Table 4 we list absorption line equivalent widths measured from spectra in the *Copernicus* U2 spectral atlas (Snow & Jenkins 1977). Uncertainties are about 20%. We have made no attempt to correct for interstellar absorption, but the largest reddening for any of the stars is $E(B-V) = 0.11$, comparable to estimates for the reddening of M31. At the *Copernicus* resolution, the 1302 Å feature is resolved into several individual lines. To compare to *IUE*, we have estimated the combined equivalent width of all the features from 1293 to 1306 Å. In most cases, we find this to be weaker than the estimates for main-sequence stars made by Welch (1982). This undermines his strongest argument that the UV emitting population must be metal-poor.

In those stars where the 1302 Å feature is weak, Si IV λ1400 is generally strong. This, combined with the absence of C IV, led Welch to consider only main-sequence stars later than B2, and thus arrive at the conclusion that the 1302 Å feature would be too strong. It is now evident from the HUT spectrum that there must be a significant contribution from hotter stars in order to produce the observed flux near the Lyman limit. Thus Welch's choice of stars for comparison is not entirely appropriate. Furthermore, a population mix over a wide range of temperatures will in general have weaker lines than individual stars, because strong lines in stars of one temperature are diluted by the light from stars of a different temperature.

To test whether the observed line strengths are *at all* compatible with a metal-rich population, we have combined the spectra of 15 Mon (O7 V) and η Uma (B4 V), convolved the sum to the HUT resolution, binned it to the HUT dispersion and measured the equivalent widths of lines measured in the HUT spectrum. We emphasize that this is not intended to be a realistic model of the stellar population, but rather a simple test to see if the line strengths really do implicate metal-poor stars. To make the exercise a bit more realistic, we have calibrated the *Copernicus* spectra to Kurucz models with $T_{\rm eff}$ = 40,000 K and $T_{\rm eff}$ = 18,000 K for 15 Mon and η UMa, respectively. A composite model where 60% of the flux in the 1350–1400 Å band comes from the cooler star and 40% from the hotter star produces a reasonable match to the continuum shape longward of 1000 Å. Thus, we added together the calibrated *Copernicus* spectra with these weights. To extend the spectrum longward of the *Copernicus* spectral range, for $\lambda > 1420$ Å we have combined *IUE* spectra of the two stars in the same proportions. The *IUE* data were obtained from the Uniform Low-Dispersion Archive (ULDA), sequences SWP8146 and SWP 32473 for 15 Mon and η UMa, respectively.

The resulting equivalent widths in the combined spectrum are shown in Table 5 and in Figure 4. The lines considered by Welch (1982) in the *IUE* spectrum all seem consistent with this simple combination of solar-metallicity main-sequence stars. The N V λ1240, C III λ1175 and C IV λ1550 features are stronger than seen in the HUT spectrum. N V is so heavily contaminated by geocoronal Lyα that we do not attach much significance to this discrepancy. On the other hand, it seems likely we would have measured large equivalent widths in M31 for C III

TABLE 4

STELLAR ABSORPTION-LINE EQUIVALENT WIDTHS IN *Copernicus* SPECTRA

Name	Type	Si IV λ1400 Equivalent Width (Å)	Si II λ1260 Equivalent Width (Å)	C II λ1335 Equivalent Width (Å)	Si II + Si III λ1302 Equivalent Width (Å)
15 Mon	07 V	2.64	1.13	1.36	1.52
10 Lac	09 V	1.97	0.59	0.60	1.40
μ Col	09.5 V	2.24	0.30	0.72	1.71
τ Sco	B0 V	4.92	0.41	0.60	1.84
42 Ori	B1 V	3.82	0.66	0.99	1.74
π Sco	B1 V	4.10	0.39	0.86	1.68
α Pav	B2.5 V	2.86	1.47	1.64	4.04
η UMa	B3 V + B4 V	1.92	2.04	2.13	2.95

TABLE 5

η UMa + 15 MONOCEROTIS ABSORPTION-LINE EQUIVALENT WIDTHS

Wavelength Feature (Å)	Stars Equivalent Width (Å)	M31 Equivalent Width (Å)
1084.....	0.78	1.4
1122.....	1.30	1.2
1175.....	1.78	0.5
1240.....	2.78	1.6
1260.....	1.27	1.5
1300.....	2.54	...
1335.....	1.47	1.3
1400.....	1.35	1.2
1550.....	2.94[a]	1.6

[a] C IV measured from *IUE* spectra.

and C IV if they were present at the strength seen in this combined stellar spectrum. There are two possible explanations other than invoking metal-poor stars, however. First, carbon may be depleted in the atmospheres of the stars producing the UV flux. This is expected for several of the populations that may contribute to the UV flux (Greggio & Renzini 1990), hot HB stars and AGB-Manqué stars in particular, which have ejected their hydrogen-rich envelopes by winds and exposed a layer that is rich in helium and nitrogen, but has very little carbon or oxygen. This is probably not in conflict with the strength of the C II 1335 Å feature, since that could be produced entirely in the intervening ISM. The other possibility is that the C III and C IV features are filled in by emission. For C IV, this is plausible from the known population of planetary nebulae discussed in § 8, but C III λ1175 is generally weak in planetary nebula spectra.

With the exception of C III and C IV, then, the absorption-line strengths in the HUT and *IUE* spectra seem to be compatible with a population of solar metallicity. However, at the signal-to-noise ratio of the HUT and *IUE* spectra, and without fitting much more detailed models for the stellar population, we do not believe that either metal-poor or more metal-rich populations can be ruled out. We interpret the weakness of the C III and C IV features as tentative evidence for carbon depletion in the atmospheres of the UV-emitting population, but without positive detection of N V or He II this conclusion remains somewhat speculative.

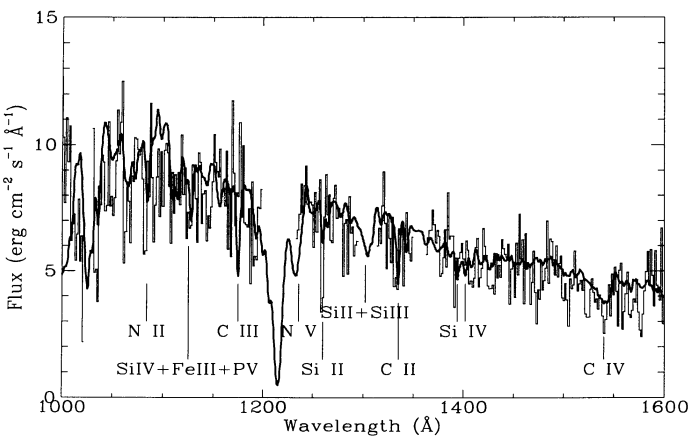

FIG. 4.—Flux-calibrated, airglow-subtracted HUT spectrum of the M31 bulge, compared to a composite spectrum of 15 Mon (O7 V) and η UMa (B3 V + B4 V), constructed from *Copernicus* spectra (calibrated using Kurucz model atmospheres) and *IUE* spectra. The histogram shows the HUT data, the solid curve the stellar spectrum. The stellar spectrum is normalized to match the mean continuum level in the HUT spectrum between 1350 and 1400 Å. Regions near the strong airglow lines in the HUT spectrum have been omitted because the noise is too great for useful comparison. The absorption features discussed in the text are marked. The abrupt change in the continuum level at 1110 Å appears to be a spurious feature in the *Copernicus* spectrum of 15 Mon, possibly due to the fact that the full spectrum is a combination of separate U2 spectrometer scans. The sharp drop at 1020 Å is also an artifact due to difficulties in normalizing the spectrum to Kurucz models where the *Copernicus* sensitivity is rapidly falling. Finally, the apparent strength of the C IV line in the observed spectrum relative to the model is misleading, because the model overestimates the continuum in this region. The measured equivalent width of the C IV line is marginally weaker in the observed spectrum. However, the coincidence of the line in the model and the data gives us additional confidence that C IV is actually detected in M31, since in both cases the feature is blue-shifted by about 8 Å relative to rest wavelengths.

6. COMPARISON TO NGC 1399

Before addressing the specific populations that might be contributing to the UV light in M31, it is interesting to compare its spectral energy distribution to that of NGC 1399. Figure 5 shows the SED ratio of M31 to NGC 1399, along with the curves that ratio should follow if the difference between the two galaxies were simply due to differences in uniform extinction following the Seaton (1979) curve. The difference in the SED's clearly cannot be due entirely to a difference in mean extinction to either galaxy, unless the extinction law is quite different from our assumed Galactic curve. Longward of 1250 Å, the spectra match reasonably well if the reddening to M31 is $E(B-V) = 0.3$ (*bottom curve*, Fig. 5). However, such a high reddening makes the difference between the intrinsic spectra of the two galaxies shortward of Lyα even more pronounced than it is in the raw data. For a quantitative comparison, we have attempted to fit a reddened NGC 1399 spectrum to the M31 data, computing χ^2 by setting the errors equal to the sum in quadrature of the fractional uncertainties from counting statistics on both spectra, multiplied by the M31

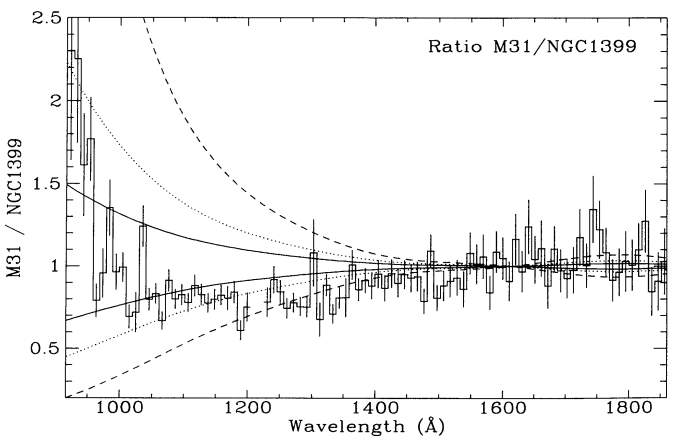

FIG. 5.—Ratio of M31 to NGC 1399 flux, normalized by the mean from 1500 to 1700 Å, after instrumental corrections and correction of the M31 flux using $E(B-V) = 0.11$. The histogram shows the data. The curves show what would be expected if the difference is simply due to a different mean extinction between the two galaxies, assuming a Seaton (1979) extinction law. The solid curve sloping downwards toward the Lyman limit shows the expected flux ratio if M31 suffers additional reddening with $\Delta E(B-V) = 0.05$ (i.e., the total reddening is $E[B-V] = 0.16$). The dotted curves are for $\Delta E(B-V) = 0.1$, and the dashed curves are for $\Delta E(B-V) = 0.2$. Curves that rise toward short wavelengths show the expected trend if M31 suffers *less* extinction than expected, or if NGC 1399 suffers more extinction. In this case $\Delta E(B-V)$ is subtracted from our nominal value of 0.11. The fact that the observed ratio does not follow any of the extinction curves suggests that the different SEDs are due to different stellar populations in the two galaxies.

flux (since we are scaling the NGC 1399 spectrum to match that flux in the mean). The best-fit is found for $E(B-V) = 0.14$, with $\chi^2 = 140$ for 75 degrees of freedom. The probability is less than 1×10^{-5} that such a high value of χ^2 would be obtained by chance if the two intrinsic spectra are the same and the extinction curve is appropriate. Even if the extinction curve is not quite right, it is unlikely that application of any reasonable extinction curve to the NGC 1399 spectrum could explain the shape of the M31 spectrum below 1000 Å. In this wavelength range, we expect the extinction to increase toward shorter wavelengths. M31, at lower galactic latitude, almost certainly suffers more attenuation than NGC 1399, so it should show a more pronounced turnover near the Lyman limit. However, even before correcting for any extinction the ratio of the mean flux between 920 and 980 Å to the flux between 1050 and 1100 Å is actually slightly *higher* in M31 than in NGC 1399 (0.61 ± 0.08 compared to 0.54 ± 0.05). LMC and SMC extinction curves are probably at least as steep as the Galactic curve in this wavelength range (Pei 1992), so such relative fluxes do not seem likely for any known extinction law.

Patchy obscuration by dust in the M31 bulge might account for part of the difference between the two spectra. We have investigated this by adding in additional components consisting of NGC 1399 spectra attenuated by various amounts of extinction. For example, assume 20% of the light leaving the M31 nucleus is reddened by $\Delta E(B-V) = 0.1$ in addition to the Galactic extinction. This will clearly produce a different SED than applying uniform reddening to the entire spectrum. Such a model produces a slightly worse fit $\chi^2/\nu = 1.94$ than the best fit for uniform Galactic extinction. We obtain a slightly better fit if we increase the fraction of light that is reddened by dust in M31 and increase the reddening of that fraction, but if that were the case the optical dust features would probably be more prominent. We have been unable to produce a good fit to the M31 spectrum even when we add in several additional components with different reddening.

We have also considered and discounted the possibility that the differences between the two spectra could be due to changes in the HUT sensitivity. The data for both galaxies were gathered over a 48 hr time span, and were reduced in the same manner. With the exception of the central few pixels of the strongest airglow lines, there is no evidence for a measurable change in HUT sensitivity during the mission from either repeated observations of the same source or comparisons to *IUE*. Pre-flight, on-orbit, and post-flight calibrations are consistent with a slow degradation in sensitivity over 3 years, varying from $\sim$0.85 to $\sim$0.65 across the first-order bandpass, and consistent with the sensitivity losses observed in laboratory measurements of the original HUT spectrograph, which was replaced after the *Challenger* accident (Davidsen et al. 1992). For the comparison here, what matters is any wavelength dependence of the variation in the HUT sensitivity, which we esimate to have been completely negligible during the mission. Thus, wavelength-dependent variations in the *ratio* of two HUT spectra must be indicative of differences in the incident spectral energy distributions. (The ratio in total fluxes, on the other hand, is significantly affected by pointing uncertainties).

A final possibility is that airglow contamination could produce a spurious excess in the M31 flux between 920 and 960 Å. There are no airglow features identified in this region in our blank sky night spectra (see, e.g., Davidsen et al. 1991, Fig. 1), but we cannot discount the possibility that weak features are present. An estimate of their possible contribution can be made by considering a HUT observation of a portion of the M31 disk taken 2 days after the M31 bulge observation. The disk observation was 1360 s long and took place mostly at night. The field was chosen for UIT, and the HUT spectrum contains virtually no signal apart from airglow. The fluxes in the airglow lines are generally lower than in the M31 bulge observation, with flux ratios varying from 1.7 to 4 for different lines. To test our sensitivity to airglow subtraction, we have scaled the M31 disk observation by factors ranging from 1/3 to 3 (times the ratio of the exposure times of the two observations), and subtracted it from the M31 bulge observation. The resultant flux in the 920–960 Å region varies by at most 17%.

We conclude that only extreme assumptions about extinction or instrument problems will allow us to reconcile the shapes of the NGC 1399 and M31 continuum. It is more likely that the remaining differences between NGC 1399 and M31 after correcting for Galactic extinction are due to differing stellar populations. In other words, *the population producing the strong UV upturn in NGC 1399 is not just more of the same population producing the mild upturn in M31.* This conclusion is important because it is independent of any preconceptions about the types of stars responsible for the UV upturn. The most obvious difference between the two galaxies is the clear excess flux in M31 near the Lyman limit. This suggests a contribution from hotter stars than those found in NGC 1399. Ferguson et al. (1991) found that, among single-temperature models, a Kurucz model of $T_{\rm eff} = 24000$ K fit the NGC 1399 SED best. Temperatures $\sim$30,000 K are preferred for M31, but single-temperature models do not fit either spectrum well. A realistic model will have stars over a wide range of temperatures in both galaxies; however, the fractional contribution from stars hotter than 30,000 K must be smaller in NGC 1399 than in M31.

It is worth commenting on the apparent deficit in the M31 continuum relative to NGC 1399 in the wavelength range 1100–1400 Å. Ignoring wavelengths shortward of 1100 Å, the M31 continuum slope is similar to that seen in 20,000 K Kurucz model atmospheres. At first glance, this suggests a significant contribution from such cooler stars to the integrated light. However, the continuum slope also resembles that of a Kurucz model with $T_{\rm eff} = 31{,}000$ K and $\log g = 3.5$. Indeed, a plot of the ratio of this model to a model with $T_{\rm eff} = 24{,}000$ K and $\log g = 4.5$ looks qualitatively similar to Figure 5. Thus the M31 continuum deficit from 1100 to 1400 Å does not uniquely implicate stars cooler than the NGC 1399 population as the dominant contributor in this wavelength range. In contrast, the excess flux near the Lyman limit virtually requires that M31 have a larger contribution from stars hotter than 30,000 K; our modelling in the next section suggests that these stars, if classical PAGB stars, contribute more than 50% of the light even at 1400 Å.

7. A TWO-COMPONENT MODEL FOR THE ULTRAVIOLET EMITTING STELLAR POPULATION IN M31

The evidence summarized in the introduction suggests that classical PAGB stars do not dominate the UV emission from elliptical galaxies with strong UV upturns. Nevertheless PAGB stars are known to be present in old metal-rich populations (as evidenced by the existence of planetary nebulae), and it is possible that they contribute significantly to the UV flux in galaxies with weaker upturns. To investigate this possibility, we

have constructed synthetic spectra of various single-mass populations of PAGB stars. Evolutionary tracks have been taken from Schönberner (1987), Wood & Faulkner (1986), and Wood (1992). From the tracks, we compute the time spent at each temperature and luminosity, and sum stellar atmosphere models in the requisite proportions. For temperatures below $T_{\rm eff} = 50{,}000$ K, we have used local thermodynamic equilibrium (LTE) model atmospheres from Kurucz (1991), while for hotter stars we have used non-LTE models from Clegg & Middlemass (1987).

There are several sources of uncertainty in the models. The chief uncertainty in the evolutionary tracks is the rate of mass-loss on and after the AGB. Different assumptions for mass loss can dramatically change the luminosity and rate of evolution of the PAGB stars. However, in the HUT range the SEDs for the different PAGB tracks (0.644, 0.598, 0.565, and 0.546 $M_\odot$ Schönberner tracks, and 0.6 and 0.7 $M_\odot$ Wood-Faulkner tracks), are similar even though different assumptions for mass loss were used. This is because all of the models evolve rapidly across the H-R diagram at nearly constant luminosity from the AGB to temperatures in excess of 80,000 K, and put out most of their luminosity while at these high temperatures. The SEDs therefore peak well beyond the Lyman limit. The second uncertainty is in the stellar model atmospheres, where two effects are important. First, the Kurucz models are computed assuming local thermodynamic equilibrium (LTE), which is not a good assumption for the hot stars considered here (Kudritzki & Hummer 1990). Second, the Kurucz models assume solar metallicity, and the Clegg-Middlemass models do not include absorption from elements heavier than helium. If the dominant UV population is metal-rich, then these models clearly underestimate the effects of line blanketing. In future papers we intend to explore the consequences of varying the metallicity in the atmospheric models. For now, we note that experiments with substituting twice solar metallicity Kurucz models produce insignificant changes in our model SED's. Finally, there are uncertainties due to interpolation along the evolutionary tracks, and interpolation into the grid of model atmospheres. However, these uncertainties are undoubtedly small compared to the uncertainties in the tracks and atmospheres themselves.

We have fit the M31 spectrum with the sum of two components, a single-mass PAGB population and the NGC 1399 SED, both attenuated by normal galactic extinction. For each model, we fit the spectrum twice, in one case allowing $E(B-V)$ to vary and in the other holding it fixed at $E(B-V) = 0.11$. The fit becomes worse for all models if we lower $E(B-V)$ beyond this value. The results of fitting are shown in Table 6. Column (1) lists the mass of the PAGB star. The letter following the mass indicates the source of the evolutionary track (Schönberner or Wood and Faulkner). Columns (2) and (3) show the goodness of fit, χ^2 and χ^2/ν, where the number of degrees of freedom ν is 74 for fixed $E(B-V)$ and 73 for variable $E(B-V)$. The extinction is indicated in column (4). Column (5) lists the production rate of PAGB stars required in the best-fit model over the area sampled by the HUT aperture. This is equivalent to the "stellar death rate" in the terminology of Greggio & Renzini (1990). The last column shows the fractional contribution of the PAGB stars to the M31 UV flux in the 1400–1450 Å band. The balance of the flux comes from the NGC 1339-like component. The best-fit model for $E(B-V) = 0.11$ is shown in Figure 6.

Much of the χ^2 discrimination between models comes from the region between 920 and 1100 Å. When the fitting range is restricted to wavelengths longer than 1100 Å, acceptable fits are achieved with 100% of the light coming from PAGB stars. However, models with 100% of the light coming from an NGC 1399-like component are still rejected.

TABLE 6

POST-ASYMPTOTIC GIANT BRANCH STAR CONTRIBUTION

Mass ($M_\odot$) (1)	χ^2 (2)	χ^2/ν (3)	$E(B-V)$ (4)	Death Rate (stars yr^{-1}) (5)	Flux Fraction at 1425 Å (6)
0.644 S	81.6	1.12	0.16	4.1×10^{-1}	0.70
0.644 S	141.1	1.91	0.11	1.3×10^{-1}	0.33
0.598 S	83.3	1.14	0.15	1.4×10^{-1}	0.68
0.598 S	117.8	1.59	0.11	8.4×10^{-2}	0.53
0.565 S	85.0	1.16	0.15	8.7×10^{-2}	0.69
0.565 S	126.5	1.71	0.11	4.4×10^{-2}	0.48
0.546 S	90.7	1.24	0.13	7.5×10^{-3}	0.47
0.546 S	103.3	1.38	0.11	8.6×10^{-3}	0.65
0.61 WF	84.7	1.16	0.20	2.9×10^{-1}	0.67
0.61 WF	162.8	2.20	0.11	1.7×10^{-2}	0.08

The conclusions are as follows. The M31 SED *can* be fitted with a component corresponding to classical PAGB stars and a component corresponding to the stars producing the UV upturn in NGC 1399. If extinction is allowed to vary, then PAGB stars contribute from 48% to 70% of the M31 flux at 1425 Å (more near the Lyman limit), and we cannot distinguish between different PAGB star masses. In all cases the fit is acceptable, so long as we sum the NGC 1399 and M31 errors in quadrature, as in § 6. If we hold $E(B-V)$ fixed, low-mass PAGB models are preferred, and may contribute up to 65% of the flux at 1425 Å. In all cases the fit is worse for fixed $E(B-V)$, and is formally excluded at the 99% confidence level for models other than 0.546 $M_\odot$. In § 9.3, below, we show that the required stellar death rate for this latter model is consistent with expectation from the population observed at optical wavelengths.

8. CONTRIBUTION FROM KNOWN PAGB STAR POPULATIONS

We now estimate the contribution to the far-UV flux from the resolved PAGB star populations in the M31 bulge, evident

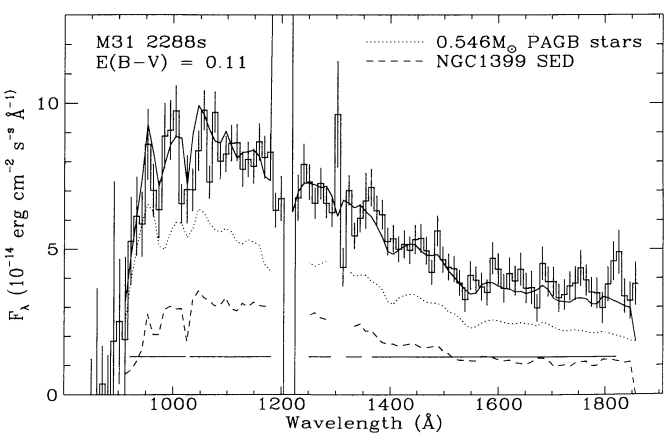

FIG. 6.—Best-fit PAGB + NGC 1399 model for the M31 spectrum. The M31 spectrum is shown, corrected for extinction assuming $E(B-V) = 0.11$. The solid curve shows the best-fit model for this extinction. The dashed curve shows the contribution from a NGC 1399-like stellar population, and the dotted curve shows the contribution from 0.546 $M_\odot$ PAGB stars.

both as planetary nebulae (PN) (Baade 1955; Ford & Jenner 1975; Ciardullo et al. 1989b) and as pointlike sources in a recent 1750 Å *HST* Faint Object Camera (FOC) image (King et al. 1992).

8.1. *Planetary Nebula Central Stars*

To estimate the number of PN, we assume the luminosity-specific PN density within 2.5 mag of the peak magnitude M^* in an [O III] λ5007 filter given by Ciardullo et al. (1989b, hereafter CJFN). We estimate an optical magnitude $V = 8.91$ in the HUT aperture from the model image discussed in § 4, converting to V-magnitude assuming $V - r = 0.2$ (Kent 1987). Comparing to Table 4 of CJFN, this then predicts there are five PN within 2.5 mag of M^* in the HUT aperture.

It is interesting to compare the expected C IV emission-line flux from such a population to the upper limit quoted in § 5. As a first approximation we assume the C IV λ1550 intensity is equal to the [O III] λ5007 flux. The peak magnitude m^* found by CJFN for the PN in M31 is 20.17. Correcting for extinction assuming $E(B-V) = 0.11$, this corresponds to a flux in [O III] of 3.9×10^{-14} ergs cm^{-2} s^{-1}. Obviously, most of the PN in the HUT slit will be fainter than m^*. Integrating 8 mag down the CJFN empirical luminosity function, normalizing so that there are five PN within 2.5 mag of m^* in the HUT slit, and applying extinction (0.9 mag at 1550 Å), the expected C IV flux is 3.2×10^{-14} ergs cm^{-2} s^{-1}. This is slightly greater than our 2 σ upper limit of 2.7×10^{-14} ergs cm^{-2} s^{-1}, but given the crude approximation and the small-number statistics involved is not in conflict with it. In spite of the uncertainties, our failure to detect C IV in emission suggests that we have not severely underestimated the number of PN in the HUT aperture.

To compute the contributions to the far-UV continuum flux, we need to assume a central star (CSPN) mass and evolutionary model, and estimate how long each PN would remain within $M - M^* < 2.5$. For consistency, we use the models of Jacoby (1989), which provide a good fit to the M31 PN luminosity function. From Jacoby's Figure 1 we can read off the time for the [O III] λ5007 luminosity to drop by a factor of 10. Dividing the number of PN in the HUT aperture by the lifetime yields a PN formation rate.[2] To estimate the UV flux, we have constructed synthetic spectra as described above from the evolutionary tracks of Wood & Faulkner (1986). While the evolutionary models are the same as used by Jacoby (1989), he used blackbodies rather than model atmospheres, so the assumptions about the SED are slightly different. The results are shown in Table 7, for different assumptions about the CSPN mass and evolutionary status. The table shows (1) the CSPN mass, (2) the assumed phase at which the star leaves the AGB, (3) the time τ for the PN to fade by 2.5 mag from the peak, (4) the PN formation rate, and (5) the mean flux in the 1400–1450 Å band. Stars labeled $\phi = 0.5$ leave the AGB between thermal pulses and are H burning. Stars labeled $\phi = 0.0$ leave the AGB during a thermal pulse and are He burning (Wood & Faulkner 1986). The 0.6 and 0.7 $M_\odot$ models are computed using individual evolutionary tracks, while the 0.61 $M_\odot$ model (Jacoby's best fit) is computed by interpolating between tracks, introducing an additional uncertainty. Jacoby's models actually constrain the CSPN mass quite tightly, but we have listed the results for other masses just to show that the contribution is small regardless of the assumed mass.

[2] This is in contrast to the arguments of Ciardullo et al. (1989b), who estimate a stellar death rate by integrating their luminosity function 8 mag down from M^* and assuming a PN lifetime of 25,000 yr. This results in a PN formation rate a factor of 5 higher than we have assumed, but based on what we consider to be somewhat shakier assumptions.

TABLE 7

PLANETARY NEBULA CENTRAL STAR CONTRIBUTION

Mass ($M_\odot$) (1)	ϕ (2)	τ (yr) (3)	Formation Rate (stars yr^{-1}) (4)	Flux at 1425 Å (ergs cm^{-2} s^{-1} Å^{-1}) (5)
0.60.....	0.0	10500	4.7×10^{-4}	1.1×10^{-16}
0.60.....	0.5	12000	4.2×10^{-4}	3.6×10^{-16}
0.70.....	0.0	5500	9.1×10^{-4}	1.5×10^{-16}
0.70.....	0.5	2000	2.5×10^{-3}	5.3×10^{-16}
0.61.....	0.0	10200	4.9×10^{-4}	1.2×10^{-16}

For the 0.61 $M_\odot$ model with an extinction $E(B-V) = 0.11$, CSPN produce 0.2%of the 1425 Å flux observed by HUT in M31. Because the PN numbers are determined in the optical, the contribution is relatively insensitive to extinction, and rises to 0.4% if $E(B-V) = 0.04$. Nevertheless the contribution to the far-UV flux within the HUT aperture from the population of PAGB stars that produce the observed PN is expected to be negligible.

8.2. *FOC Pointlike Sources*

Early observations of M31 with *HST* have revealed a large number of pointlike sources, superposed on a smooth background (King et al. 1992). In observations with the Faint Object Camera (FOC), 137 sources were detected in a 44″ × 44″ field of view through a wide-bandpass filter (F175W) centered at ~1750 Å. The point sources are most likely PAGB stars. However, problems with calibrating the sensitivity of the FOC and the redleak in the F175W filter make it difficult to determine their contribution to the total far-UV flux from the FOC image alone. By comparing to the HUT data, we can make a rough estimate of the point-source contribution if we assume that their spatial distribution follows the optical luminosity profile. The total count rate from the point sources in the FOC field is 70.3 counts s^{-1}, corresponding to a 1750 Å flux of $\sim 5.3 \times 10^{-15}$ ergs cm^{-2} s^{-1} Å^{-1} (King et al. 1992), using the nominal FOC sensitivity. This rate should be relatively insensitive to redleak, since the resolved sources are believed to be very hot. From the optical profile, we estimate that 65 sources would be included in the HUT aperture, producing a flux of 2.4×10^{-15} ergs cm^{-2} s^{-1} Å^{-1}. The number is virtually unchanged (64 sources) when we do the computation using the UIT 1520 Å surface-brightness profile. The HUT flux at 1725 Å from Table 2 is 1.66×10^{-14} ergs cm^{-2} s^{-1} Å^{-1}. (Integrating a combined HUT + scaled *IUE* SED out to 2125 Å through the bandpass of the FOC F175W gives a mean flux of 1.59×10^{-14} ergs cm^{-2} s^{-1} Å^{-1}.) Thus the point sources account for ~15% of the HUT 1750 Å flux. This comparison with the HUT flux is in good agreement with the contribution estimated by King et al. (1992) from comparison of the FOC results to the *IUE* data.

This can be interpreted as a *lower* limit on the PAGB star contribution to the M31 far-UV flux. First, the UV sensitivity of the FOC *f*/48 mode on orbit is uncertain. Therefore the contribution from the *detected* point sources could be greater than calculated above (Buson 1992; Bertola 1992). Second, using Kurucz-model atmospheres we find that for stars of fixed bolometric luminosity the flux in the FOC F175W filter peaks

at $T_{\rm eff} \sim 18{,}000$ K. At this temperature, the PAGB stars are evolving rapidly, and drop below the FOC detection limit within a fraction of the time spent at high luminosities. For example, a 0.598 $M_\odot$ PAGB star stays within 2 mag of its peak FOC flux for only 4×10^3 yr, while it stays within 2 mag of its peak *bolometric* luminosity for 10^4 yr. Thus even for a *single mass* population of PAGB stars, we expect both a diffuse component and a resolved component in FOC far-UV images. The relative contribution of each of these to the *total* far-UV flux depends on the mass of the PAGB star population, the point-source detection limit of the FOC, possible contributions from planetary-nebula emission lines, and the extent to which dust left over from mass-loss on the AGB attenuates the emission from the stars in the FOC bandpass. The most straightforward estimate, ignoring dust and emission lines, suggests that the total expected flux in the diffuse component from a 0.55 to 0.6 $M_\odot$ PAGB star population would be much fainter than the far-UV portion of the diffuse component inferred from the FOC data using the nominal calibration.

It is interesting to note that the number of FOC point sources per unit area in the M31 bulge is much higher than the number of planetary nebulae per unit area inferred from the optical counts. With the peak of the F175W response function at a temperature of 18,000 K, we do not *expect* a one-to-one correspondence between planetary nebulae (whose central stars generally have temperatures in excess of 50,000 K) and point sources. Nevertheless, the disparity in counts is noteworthy since for stars on the Schönberner (1983) tracks the time spent in the planetary nebula phase is *longer* than the time spent near the peak of the FOC F175W filter response. This suggests that the FOC point sources are unlikely to be cooler progenitors of the observed planetary nebula population. The most likely interpretation is that the majority of the FOC pointlike sources are low-mass PAGB stars that either produce faint PN or miss the planetary nebula phase entirely because of their slow evolution.

With the nominal FOC calibration used by King et al. (1992), the detected point sources produce only a small fraction of the 1750 Å flux, but it is plausible that the low-mass (0.546 $M_\odot$) PAGB stars in our best-fit composite model of the spectral-energy distribution fall below the FOC point source detection limits. If the FOC is less sensitive in the far-UV, the 65% share could be accounted for by the resolved sources, but they would have to be higher mass PAGB stars. It seems unlikely that the nominal FOC sensitivity and redleak calibrations could be so far off that the resolved sources produce *all* of the far-UV flux. The mean point source density in the King et al. observation is 0.07 arcsec^{-2}. If these sources account for the total flux, then a few would have been detected, or at least a mottled appearance noted, in the UIT observations (O'Connell et al. 1992), which do not suffer from redleak and have a FWHM in the point-spread function of $\sim 3''$. Translated to the UIT magnitude system, the 65 FOC sources in the HUT aperture would each have to have $m_{152} \sim 17.8$ if the sources account for the total flux measured by HUT at 1520 Å. The point source detection limit in the UIT image was $m_{152} \sim 18.4$, and the source density is low enough in the outer regions that crowding would not have been a problem. Hence, given the current calibration uncertainties, the FOC results appear to be consistent with our composite model of the spectral energy distribution. It will be important to obtain a better calibration of the UV sensitivity of the FOC, as detailed modeling of the luminosity function of the resolved sources could provide important constraints on the mass distribution of the PAGB star population and test our inferences from the spectral fitting.

9. DISCUSSION

9.1. *Evidence for a Composite Population*

The most important conclusion to be drawn from the preceding sections is that PAGB stars exist over a range of masses in the M31 bulge. The evidence to support this conclusion is as follows

1. The far-UV continuum flux expected from the known planetary-nebula population (thought to have central-star masses of $\sim 0.6\ M_\odot$) falls short of the observed flux by more than two orders of magnitude.

2. Comparison of the NGC 1399 and M31 SEDs suggests a simple model in which the stars producing the strong UV upturn in NGC 1399 exist in M31, but in smaller proportion compared to classical PAGB stars.

3. With $E(B-V)$ fixed at 0.11, the best fit for such a two-population model requires 65% of the flux at 1425 Å from 0.546 $M_\odot$ hydrogen-burning PAGB stars, and the rest from the NGC 1399-like population. The fits are significantly worse for higher mass PAGB star populations, unless the extinction is greater than generally assumed.

4. The point source density in the FOC images of the M31 bulge is much higher than the planetary nebula density. The most likely interpretation is that the FOC is detecting low-mass PAGB stars, which produce faint PN or skip the PN phase entirely due to their slow evolution to high temperatures.

These arguments suggest that the high-mass (0.6 $M_\odot$) PAGB stars sampled by the known planetary nebulae are the tail of a distribution that extends to lower mass. A spread in evolved-star mass is expected due both to an intrinsic spread in the metallicity and age of the progenitor population, and to the stochastic process of mass loss on the RGB and AGB. The spread of HB masses in globular clusters is evidence that such stochastic processes are important. Nevertheless, the locus of HB and post-HB star masses must be determined by parameters such as metallicity, age, and/or helium enrichment. It is plausible, therefore, that the UV rising branches in M31 and NGC 1399 are due to stars that are all in post-HB phases of evolution, but the mix of masses is different in the two galaxies due to the different mean metallicities, or possibly ages, of the two systems.

In the simplest scenario (Larson 1974; Vader 1986; Arimoto & Yoshii 1987; Matteucci & Tornambè 1987; Brocato et al. 1990), both M31 and NGC 1399 form most of their stars fairly rapidly at an early epoch. Chemical evolution produces a wide spread in metallicity in the populations of both galaxies, but, due to its deeper potential, NGC 1399 retains more metals and reaches a higher enrichment than M31. Most of the *optical* light in the M31 bulge and NGC 1399 comes from stars with metallicities higher than solar. However, because the durations of different phases of stellar evolution depend on metallicity (and helium abundance), the current post-HB evolution of stars could be quite different in the two galaxies. Stars at or below solar metallicity will tend to evolve through the classical AGB and PAGB phases, since we see such stars in the disk and bulge of our own galaxy. Stars with higher metallicity may either become low-mass PAGB stars (Burstein et al. 1988; Bertelli et al. 1989), they may leave the AGB early and become

PEAGB stars, or they may skip the AGB entirely (AGB-Manqué stars) and evolve to high temperatures directly from the horizontal branch (Greggio & Renzini 1990; Brocato et al. 1990; Castellani & Tornambè 1991; Castellani, Limongi, & Tornambè 1992; Horch et al. 1992). In any case, these candidates produce more UV photons over their lifetimes than the classical high-mass PAGB stars that come from the lower-metallicity population. Within the classical PAGB star class, the trend toward higher UV efficiency with decreasing mass is accompanied by a trend toward lower peak temperatures. This trend continues for PEAGB stars and AGB-Manqué stars (for example, in the 0.48 $M_\odot, Z = 0.02$ model of Castellani & Tornambè 1989 most of the UV light is emitted while stars are at a temperature $T_{\rm eff} \sim 25{,}000$ K), although some models show quite complicated behavior in the L–$T_{\rm eff}$ plane (Castellani & Tornambè 1991; Horch et al. 1992). *The trend toward stronger UV rising branches with increasing mean metallicity is thus accompanied by a trend toward lower characteristic temperature, which is just what we find when comparing M31 to NGC 1399.* We stress however, that because of the intrinsic metallicity *spread* in the stellar populations and stochastic variations from star to star in the amount of mass shed on the giant branches, the far-UV emitting population in both galaxies is undoubtedly a mixture of the different post-RGB, EHB, and post-HB types.

We should note that this scenario is not unique in its ability to explain the far-UV properties of M31 and NGC 1399. In particular, relaxing the requirement that all the stars in both galaxies have roughly the same age could produce similar results. If the old metal-rich population in M31 were accompanied by a younger metal-rich population that is *not* present in NGC 1399, PAGB stars of a range of masses would also be present, and the trends in both the HUT spectra and the variation of UV-optical color with metallicity (since Mg_2 is sensitive to age as well as metallicity) might be reproduced. However, since a metallicity spread must *undoubtedly* exist due to chemical evolution, while there is no unambiguous evidence for the existence of a young or intermediate-age population, we suspect that metallicity rather than age controls the far-UV properties of present-day ellipticals and spiral bulges.

9.2. *Implications for the Planetary Nebula Population*

In the scenario just outlined, wherein the distribution of HB and post-HB star mass is governed by metallicity, most of the far-UV flux in a galaxy with a strong UV-upturn comes from stars that would *not* go through a bright planetary-nebula phase. In the slowly evolving post-HB phases discussed above, a surrounding nebula would probably disperse before the ionizing flux becomes large enough to produce observable emission lines. The objects are also intrinsically much fainter. Nevertheless, bright planetary nebulae will exist even in galaxies with the strongest UV upturns, because of the spread in metallicity and mass loss within the stellar population. The planetary nebulae detected in high-metallicity systems such as NGC 1399 probably sample the low-metallicity, high-mass tail of the PAGB/PEAGB/AGB-Manqué star mass distribution. However, an increase in the number of low-mass PEAGB or AGB-Manqué stars in a galaxy with a strong UV upturn must be accompanied by a *decrease* in the population of higher mass classical PAGB stars and therefore also a decrease in the relative number of planetary nebulae. From this scenario we then predict that as the UV/optical flux ratio *increases*, the number of PN per unit bolometric luminosity should *decrease*.

This prediction can be tested with data already in the literature. PN counts for NGC 1399 have not been published, but a careful census of planetary nebulae in several elliptical galaxies and spiral bulges has been carried out in an effort to measure the Hubble constant (Ciardullo et al. 1989b; Ciardullo, Jacoby, & Ford 1989a; Jacoby et al. 1989; Jacoby, Ciardullo, & Ford 1990). Figure 7 shows the variation in the luminosity-specific PN density $\alpha_{2.5}$ with 1550 Å $- V$ color based on these data (see also Ciardullo et al. 1991). The trend is exactly as predicted. The galaxy with the largest number of PN per unit luminosity is M32, which has the weakest far-UV component yet measured (Buson et al. 1990). The galaxy with the smallest number of PN per unit luminosity is NGC 4649, which has one of the strongest UV upturns known (Bertola et al. 1982), comparable to that of NGC 1399 (Burstein et al. 1988). Incompleteness at the greater distance of NGC 4649 is unlikely to explain this trend, as several other galaxies at the same distance are observed to have high values of $\alpha_{2.5}$.

We should also expect to see $\alpha_{2.5}$ *increase* with radius in giant ellipticals, as metallicity generally decreases with radius. Unfortunately, searching for such a trend is difficult because PN become hard to detect against the high-surface-brightness background near the centers of elliptical galaxies. All of the galaxies in the Virgo Cluster sample (Jacoby et al. 1990) show a deficit of PN near the center, but without carefully estimating the detectability of PN against the Galaxy background, it is impossible to tell whether the deficit is real or simply the result of incompleteness. Jacoby et al. (1990) used the radial distribution of PN to *correct* $\alpha_{2.5}$ for incompleteness. However, if the PN are *really* depleted in the centers of the galaxies as opposed to being just too hard to detect, then $\alpha_{2.5}$ may be still lower in the UV-bright galaxies.

A further prediction of this hypothesis is that in metal-rich populations, the heavy-element abundances in PN should be lower than the mean for the stellar population. This may account for the otherwise puzzling observation that planetary

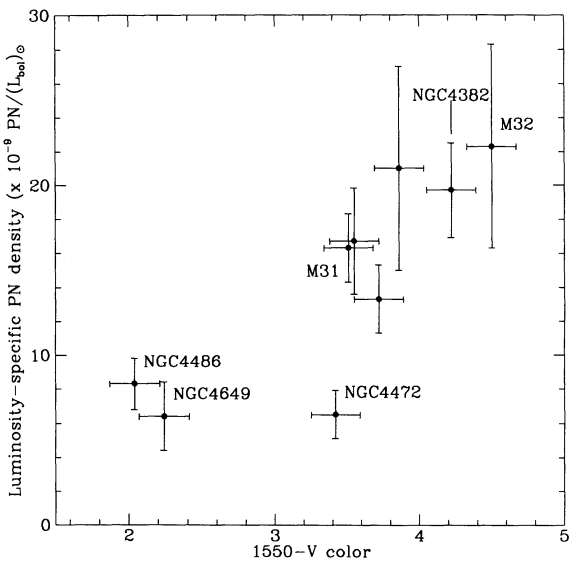

FIG. 7.—Variation in the number of planetary nebulae per unit luminosity with strength of the UV upturn. PN densities are from best-fits to the planetary nebula luminosity function, integrated 2.5 mag down from the characteristic magnitude M^* (Ciardullo et al. 1989a, b; Jacoby et al. 1989). Error bars are as quoted in these references, or read from the plots. The 1550 Å $- V$ colors are from Burstein et al. (1988). Selected galaxies are labeled.

nebulae in the Galactic bulge have near solar oxygen abundances (Ratag 1991), even though the abundance distribution for K giants peaks at [Fe/H] $\sim +0.3$ (Rich 1988).

9.3. *The Relation Between the SED Shape and the Strength of the UV upturn*

Let us consider again the results of fitting two components to the spectrum of M31. With $E(B-V) = 0.11$ the best fit was found for a classical PAGB contribution of 65% at 1425 Å, with the rest of the flux coming from an NGC 1399-like component, which we hypothesize are lower mass, metal-rich EHB or post-HB stars. In fitting only two components to the M31 spectrum we are obviously oversimplifying the true situation. However, we can still ask whether the relative UV fluxes of NGC 1399 and M31 are roughly consistent with what we expect from the different contributions of the two components. To make the comparison, we must compute the UV-to-optical flux ratios for M31 and NGC 1399. For NGC 1399 the V-magnitude in the HUT aperture is 11.51, which we derive from the photometry of Franx, Illingworth, & Heckman (1989), fixing the zero point to Burstein et al. (1988). Comparing this to the HUT flux, we find a 1425 Å to V-band flux ratio of $f_{1425}/f_{5500} = 0.14$. After correction for extinction, the optical photometry of M31 gives $V = 8.54$ in the HUT aperture, and the 1425 Å to V-band flux ratio is thus $f_{1425}/f_{5500} = 0.038$. Assuming the main-sequence-turnoff luminosities and colors are similar for the progenitors of PAGB stars and the lower mass objects, we can compute the expected ratio $R = f_{1425}/f_{5500}$ for the composite M31 population from the following equation

$$R = pR_p + (1 - p)\eta R_p , \quad (1)$$

where p is the fraction of the main-sequence population that evolves into PAGB stars, R_p is the UV/optical flux ratio for that population, and η is the ratio of the number of UV photons produced per star in the NGC 1399-like population to that in the PAGB population. Since the PAGB stars are less efficient far-UV emitters, p must be between 0.65 and 1.0 in order to produce the 65% of the far-UV flux required by our best-fit model. Taking $p = 0.85$, for example, we find $\eta = 7$ would be required to produce the observed values of R for both M31 and NGC 1399. This is within the range expected if the bulk of the far-UV emission in NGC 1399 comes from AGB-Manqué stars (see Castellani & Tornambè 1991, Figs. 7 and 8).

A related question is whether a population of 0.546 $M_\odot$ PAGB stars can produce 65% of the M31 1425 Å flux, given a theoretical estimate of the stellar death rate. Greggio & Renzini (1990) estimate a stellar death rate (PAGB star production rate) of 0.6 stars yr^{-1} for the total bulge of M31, which they assume has a B-band absolute magnitude of $M_B = -19.85$. The integrated absolute magnitude in the HUT slit is $M_B = -14.96$ (taking $B-V = 0.93$), but given the different sources of photometry, a zero-point difference of up to 0.5 mag is not inconceivable. The implied stellar death rate in the HUT slit is 6.6×10^{-3} stars yr^{-1}. For the best-fit model with $M = 0.546\ M_\odot$ and $E(B-V) = 0.11$, the implied stellar death rate is 8.6×10^{-3} stars per year. These agree to within 30%, which is well within the uncertainties. (In contrast, a model where the far-UV emission is produced by 0.598 $M_\odot$ PAGB stars would require a death rate of 8.5×10^{-2} stars yr^{-1}, well above the theoretical prediction; but such a model does not match the SED very well either if $E[B-V] = 0.11$.) The stars in the NGC 1399-like component probably do not add significantly to the required death rate, because they produce many more UV photons per star and thus fewer stars are needed.

These arguments add support to our interpretation of the M31 spectrum. By analyzing the *shape* of the spectrum, we arrived at a model that adequately predicts the UV/optical flux ratio. Furthermore, the required stellar death rate of the best-fit model is in reasonable agreement with expectations from theory. If we take the small *discrepancy* between the predicted and required stellar death rates at face value, it suggests that PAGB or PEAGB stars with masses less than 0.546 $M_\odot$ contribute to the M31 spectrum. Such stars would be both cooler and more efficient producers of UV photons than the stars considered in our model fitting (Brocato et al. 1990; Castellani & Tornambè 1991). Therefore, including such an intermediate population might produce both a better fit to the M31 spectrum and eliminate the problem of needing too many PAGB stars. Now that evolutionary tracks are available for the post-horizontal branch evolution of metal-rich stars (Castellani & Tornambè 1991; Horch et al. 1992), it should be possible to produce more realistic models (Ferguson & Davidsen 1993).

Our interpretation of the far-UV SEDs of NGC 1399 and M31 translates into several specific predictions for M32, a galaxy with a very weak far-UV upturn. Because the mean metallicity is lower than in M31, M32 should have more classical PAGB stars per unit mass than M31. The implications are as follows

1. M32 should show proportionately more flux near the Lyman limit than M31. In the sub-Lyα region, we expect that PAGB models will provide a reasonably good match to the M32 SED. This prediction can be tested by HUT observations during the Astro-2 mission.
2. There should be more planetary nebulae per unit stellar mass in M32 than in M31. This is in agreement with existing data, but could be further constrained with more complete surveys.
3. If the point sources seen in M31 with the FOC are classical PAGB stars, similar sources should be detected in M32, and their combined flux relative to the total in the diffuse component should be *greater* than in M31.

It is also worth commenting on the curious observation from UIT (O'Connell et al. 1992) that M32 becomes *bluer* (in 1520 Å to 2490 Å flux ratio) with increasing radius from the center, while M31 and NGC 1399 become *redder*. This may indicate that in M32 the contribution from metal-poor blue horizontal branch stars (which must be present at some level) is becoming significant, especially at large radii, a suggestion previously put forward by Barbaro & Olivi (1989). The characteristic temperature of such a population would be much cooler than a PAGB star population, and the M32 SED at large radii should then look more like the HUT spectrum of M79 (Davidsen & Ferguson 1992) than M31 or NGC 1399.

In metal-rich galaxies such as NGC 1399, it is the lowest mass stars that produce most of the far-UV upturn. Therefore, the strength of the UV upturn should increase rapidly with time as stars with masses less than 0.5 $M_\odot$ begin to dominate the post-RGB evolution in a galaxy. This results in a spectral evolution with lookback time significantly different from that predicted by models where the UV upturn is assumed to be due to continuing star formation. In our scenario (see also Greggio & Renzini 1990), the UV upturn in giant ellipticals should weaken substantially with increasing lookback time or redshift. At the same time, the characteristic temperature of the

UV-emitting population should increase, reflecting a larger relative contribution of higher-mass PAGB stars. These predictions could potentially be tested with long *HST* observations of the SED's of luminous elliptical galaxies at redshifts of a few tenths.

10. SUMMARY AND CONCLUSIONS

The far-ultraviolet spectrum (912–1850 Å) of the bulge of M31 has been observed with a signal-to-noise ratio of about 10 at 3 Å resolution with the Hopkins Ultraviolet Telescope. Several absorption lines are detected, while no emission lines are seen (other than those due to the Earth's airglow). From 1300 to 1800 Å the M31 SED is very similar to that obtained previously with *IUE*, and the ratio of the flux measured through the $9''.4 \times 116''$ HUT aperture to the rounded $10'' \times 20''$ *IUE* aperture is consistent with the far-UV surface-brightness profile measured by UIT.

Without computing detailed models of the stellar population, it is difficult to draw inferences about the metallicity of the stellar population from the line strengths observed in the HUT spectrum. Our simple comparisons to *Copernicus* and *IUE* spectra suggest that metal-rich stars *are* allowed, a result at variance with the conclusions of Welch (1982). The most significant discrepancies from our combination of solar-metallicity main-sequence stars is the weakness of the C III λ1175 and C IV λ1550 lines in the M31 spectrum, suggesting that the hot stars producing the far-UV emission may be depleted in carbon, if not in other metals.

A comparison of the HUT spectrum of M31 to that of NGC 1399, a normal elliptical with a very strong UV upturn, reveals differences that are not attributable to uncertainties in the extinction toward the two galaxies. M31 has proportionately more flux near the Lyman limit, indicating a larger contribution from hot stars ($T_{\rm eff} > 25{,}000$ K) than in NGC 1399.

We have constructed a simple two-component model to simulate the actual distribution of evolving UV-bright stars in M31. If we assume the hotter component is due to PAGB stars following the Schönberner (1983) tracks, then, for our adopted extinction, the best fit to our spectrum attributes 65% of the flux at 1425 Å to the PAGB component and 35% to the NGC 1399-like component. Similarly good fits, with similar fractional contributions from the two components, are obtained for higher-mass PAGB stars if we allow the reddening to be larger than $E(B-V) = 0.11$. However, only the lowest mass tracks ($0.546\ M_\odot$) yield a PAGB-star death rate low enough to be consistent with the theoretically expected value for M31 (Greggio & Renzini 1990), and a best-fit extinction consistent with previous estimates in the literature.

The contribution to the far-UV flux from the *known* population of PAGB stars, sampled by the planetary nebulae, is estimated to be less than 1% at 1425 Å. The contribution from the pointlike sources detected with the *HST* FOC (King et al. 1992; Buson 1992), *inferred* to be low-mass PAGB stars, is $\sim$15% if the nominal FOC calibration assumed by King et al. (1992) is correct, but could be much higher if the FOC UV sensitivity is much lower than expected. For reasons stated in § 8.2, it appears unlikely that the FOC point sources account for all of the far-UV flux in M31. The FOC PAGB stars, possibly along with somewhat lower mass, lower luminosity PAGB stars that are fainter than FOC detection limit, may thus be identified with the PAGB component of the M31 SED required to fit the HUT spectrum.

In the model we envision, the cooler NGC 1399-like component of the M31 SED may be identified with even lower mass, higher metallicity stars in the EHB, PEAGB, or AGB-Manqué phase. The NGC 1399 SED is extremely well fit, for example, by stars evolving along the $0.48\ M_\odot$, $Z = 0.02$ (solar metallicity) track of Castellani & Tornambè (1991) (Davidsen & Ferguson 1992). These stars produce much more far-UV radiation over their lifetimes than do the more massive PAGB stars, and can therefore provide the flux observed in the elliptical galaxies with the strongest UV upturns, such as NGC 1399.

We thus arrive at the conclusion that the far-UV upturns of spiral bulges and elliptical galaxies are produced by a mixture of EHB and/or post-HB stars with a distribution of masses and metallicities determined by the early chemical enrichment history of each galaxy and subsequent stellar evolution. Following Greggio & Renzini (1990), we propose that galaxies with the strongest UV upturns are dominated by a large contribution from very low-mass EHB, PEAGB, or AGB-Manqué stars, while galaxies with weak UV upturns are dominated by higher mass, lower metallicity classical PAGB stars, which are less efficient producers of far-UV radiation. The M31 bulge is an intermediate case, where there are significant contributions from all these stars.

This scenario provides a natural explanation of the correlation of the strength of the UV upturn of a galaxy with its mean metallicity, since galaxies with higher metallicity will have a higher proportion of low-mass EHB and post-HB stars. This results in testable predictions (see § 9.3) for the far-UV SEDs of metal-poor galaxies and for the spectral evolution of giant ellipticals.

The scenario proposed above also seems consistent with several independent measures of the evolved star population. Specifically, it predicts that the number of planetary nebulae per unit luminosity should decrease as the strength of the UV upturn increases, since PN are produced by the high-mass PAGB star population. A strong correlation of this type is in fact found in existing data. In addition, since the planetary nebulae in this scenario sample the low-Z tail of the metallicity distribution in metal-rich populations, the heavy-element abundances are expected to be lower than the mean for the total stellar population. This prediction is supported by PN abundance measurements in the Galactic bulge (Ratag 1991).

The next step in testing this general framework is to construct more realistic composite models of eliptical galaxy SEDs that incorporate the expected metallicity distributions in the stellar populations (rather than the simple two-component model we have assumed), and that follow stars through the appropriate post-RGB phases for their ages and metallicities (Ferguson & Davidsen 1993). Comparing both the fluxes and SEDs of such composite PAGB/EHB/PEAGB/AGB-Manqué populations with HUT, *IUE*, and *HST* observations will provide a crucial test of the stellar evolution models, and may ultimately help constrain the metallicity spread in elliptical galaxies. There is some hope, then, that the UV upturn will soon cease to be a puzzle and will become instead a useful tool for probing galaxy evolution.

We are extremely grateful to our colleagues on the HUT science team, and to the staffs of The Johns Hopkins University Applied Physics Laboratory, NASA's KSC, JSC, GSFC, and MSFC centers, and NASA Headquarters for their

perseverance in the face of the many challenges that confronted the Astro-1 mission. Thanks are also due to Robin Clegg and Robert Kurucz for providing computer-readable spectra from their model atmospheres; to Peter Wood for providing further information on PAGB-star evolutionary tracks; to Ivan King for discussing the FOC results prior to publication and for commenting on the manuscript; and to Robert O'Connell for providing the UIT photometry prior to publication, and for providing valuable comments as referee. This paper has made use of the NASA/IPAC Extragalactic Database (NED) which is operated by the Jet Propulsion Laboratory, California Institute of Technology, under contract with the National Aeronautics and Space Administration, and the SIMBAD data base, operated at CDS, Strasbourg, France. The HUT project is supported by NASA contract NAS5-27000 to The Johns Hopkins University. H.C.F. acknowledges research support from the UK Science and Engineering Research Council.

REFERENCES

Arimoto, N., & Yoshii, Y. 1987, A&A, 173, 23
Baade, W. 1955, AJ, 60, 151
Barbaro, G., & Olivi, F. M. 1989, ApJ, 337, 125
Bertelli, F., Chiosi, C., & Bertola, F. 1989, ApJ, 339, 889
Bertola, F. 1992, private communication
Bertola, F., Capaccioli, M., & Oke, J. B. 1982, ApJ, 254, 494
Bohlin, R. C., Cornett, R. H., Hill, J. K., Hill, R. S., O'Connell, R. W., & Stecher, T. P. 1985, ApJ, 298, L37
Brocato, E., Matteucci, F., Mazzitelli, I., & Tornambè, A. 1990, ApJ, 349, 458
Bruzual, G. 1983, ApJ, 273, 105
Burstein, D., Bertola, F., Buson, L. M., Faber, S. M., & Lauer, T. R. 1988, ApJ, 328, 440
Buson, L. M. 1992, presented at Science with the *Hubble Space Telescope* (Sardinia), unpublished
Buson, L. M., Bertola, F., & Burstein, D. 1990, in Windows on Galaxies, ed. G. Fabbiano, J. S. Gallagher, & A. Renzini (Dordrecht: Kluwer), 759
Castellani, M., Limongi, M., & Tornambè, A. 1992, ApJ, 389, 227
Castellani, M., & Tornambè, A. 1991, ApJ, 381, 393
Ciardullo, R., Jacoby, G. H., & Ford, H. C. 1989a, ApJ, 344, 715
Ciardullo, R., Jacoby, G. H., Ford, H. C., & Neill, J. D. 1989b, ApJ, 339, 53 (CJFN)
Ciardullo, R., Jacoby, G. H., & Harris, W. E. 1991, ApJ, 383, 487
Clegg, R. E. S., & Middlemass, D. 1987, MNRAS, 228, 759
Code, A. D., & Welch, G. A. 1979, ApJ, 228, 95
Davidsen, A. F., & Ferguson, H. C. 1993, in The Physics of Nearby Galaxies: Nature or Nurture? ed. T. X. Thuan & C. Balkowski (Gif-sur-Yvette: Editions Frontières), in press
Davidsen, A. F., et al. 1991, Nature, 351, 128
———. 1992, ApJ, 392, 264
de Boer, K. S. 1982, A&AS, 50, 247
Deharveng, J. M., Joubert, M., Monnet, G., & Donas, J. 1982, A&A, 106, 16
Ferguson, H. C., & Davidsen, A. F. 1993, in preparation
Ferguson, H. C., et al. 1991, ApJ, 382, L69
Ford, H. C., & Jenner, D. C. 1975, ApJ, 202, 365
Franx, M., Illingworth, G., & Heckman, T. 1989, AJ, 98, 538
Greggio, L., & Renzini, A. 1990, ApJ, 364, 35
Horch, E., Demarque, P., & Pinsonneault, M. 1992, ApJ, 388, L53
Iben, I., & Renzini, A. 1983, ARA&A, 21, 271
Jacoby, G. H. 1989, ApJ, 339, 39
Jacoby, G. H., Ciardullo, R., & Ford, H. C. 1990, ApJ, 356, 332
Jacoby, G. H., Ciardullo, R., Ford, H. C., & Booth, J. 1989, ApJ, 344, 704
Jedrzejewski, R. 1987, MNRAS, 226, 747
Johnson, H. M. 1979, ApJ, 230, L137
Kent, S. M. 1983, ApJ, 266, 562
———. 1987, AJ, 94, 306
Kimble, R. A., Davidsen, A. F., Long, K. S., Bowers, C. W., Kriss, G. A., Finley, D. S., & Koester, D. 1993, Proc. 10th Internat. Colloq. on UV and X-ray Spectroscopy of Astrophysical and Laboratory Plasmas, ed. S. M. Kahn & E. H. Silver (Cambridge: Cambridge Univ. Press) in press
King, I., et al. 1992, ApJ, 397, L35
Kudritzki, R. P., & Hummer, D. G. 1990, ARA&A, 28, 303
Kurucz, R. L. 1991, CfA preprint no. 3181
Larson, R. B. 1974, MNRAS, 169, 229
Longo, R., Stalio, R., Polidan, R. S., & Rossi, L. 1989, ApJ, 339, 474
Matteucci, F., & Tornambè, A. 1987, A&A, 185, 51
McClure, R. D., & Racine, R. 1969, AJ, 74, 1000
Mochkovitch, R. 1986, A&A, 157, 311
Nørgaard-Nielsen, H. U., & Kjaergaard, P. 1981, A&A, 93, 290
O'Connell, R. W. 1991, in Stellar Populations in Galaxies, ed. A. Renzini & B. Barbuy (Dordrecht: Kluwer), 233
———. 1992, private communication
O'Connell, R. W., et al. 1992, ApJ, 395, L45
Pei, Y. C. 1992, Princeton preprint
Perola, G. C., & Tarenghi, M. 1980, ApJ, 240, 447
Ratag, M. 1991, Ph.D. thesis, Leiden Univ.
Rich, M. 1988, AJ, 95, 828
Rocca-Volmerange, B., & Guiderdoni, B. 1987, A&A, 175, 15
Sandage, A. 1988, ARA&A, 26, 561
Schönberner, D. 1983, ApJ, 272, 708
———. 1987, in Planetary Nebulae, ed. S. Torres-Peimbert (London: IAU). 340
Seaton, M. J. 1979, MNRAS, 187, 75P
Snow, T. P., Jr., & Jenkins, E. B. 1977, ApJS, 33, 269
Snow, T. P., Jr., & Morton, D. C. 1976, ApJS, 32, 429
Tully, R. B. 1988, Nearby Galaxies Catalogue (Cambridge: Cambridge Univ. Press)
Vader, J. P. 1986, ApJ, 305, 669
Walborn, N. R., Nichols-Bohlin, J., & Panek, R. J. 1985, NASA Ref. Pub. 1115
Welch, G. A. 1982, ApJ, 259, 77
Wood, P. R. 1992, private communication
Wood, P. R., & Faulkner, D. J. 1986, ApJ, 307, 659
Yoshii, Y., & Takahara, F. 1988, ApJ, 326, 1